



# OPEN A study of dynamic functional connectivity changes in flight trainees based on a triple network model

Lu Ye<sup>1</sup>, Liya Ba<sup>1</sup> & Dongfeng Yan<sup>1</sup>✉

The time-varying functional connectivity of the Central Executive Network (CEN), Default Mode Network (DMN), and Salience Network (SN) in flight trainees during a resting state was investigated using dynamic functional network connectivity (dFNC). The study included 39 flight trainees and 37 age- and sex-matched healthy controls. Resting-state fMRI data and behavioral test outcomes were obtained from both groups. Independent component analysis (ICA), sliding window, and K-means clustering approaches were utilized for evaluating functional network connectivity (FNC) and temporal metrics based on the triple networks. Correlation analyses were performed on the behavioral assessments and these metrics. The flight trainees demonstrated a significantly enhanced functional connection linking the CEN and DMN in state 2 ( $P < 0.05$ , FDR corrected). Additionally, flight trainees spent less time in state 5, while they exhibited a protracted mean dwell time and fractional windows in state 2, which were significantly correlated with accuracy on the Berg Card Sorting Test (BCST) and Change Detection Test (all  $P < 0.05$ ). The improved connectivity of flight trainees between the CEN and DMN following the completion of rigorous flight training resulted in increased stability. This enhancement may be relevant to cognitive abilities such as decision-making, memory, and information integration. When multitasking, flight trainees displayed superior visual processing skills and enhanced cognitive flexibility. dFNC research provides a unique perspective on the sophisticated cognitive capabilities that are required in high-demand, high-stress occupations such as piloting, thereby providing significant insights into the intricate brain mechanisms that are inherent in these domains.

**Keywords** Flight trainees, Resting-state fMRI, Dynamic functional network connectivity, Independent component analysis

In recent years, the swift advancement of the global civil aviation sector has made air transportation a crucial catalyst for economic growth in several nations and areas while simultaneously confronting unparalleled safety difficulties. Civil aviation safety, fundamental to the sustainable and robust advancement of the sector, is intricately linked to the unwavering dedication of every aviation professional. The extensive implementation of technical advancements and automated technologies has progressively converted pilots from conventional operators to essential monitors of the complete flight system in real time. This transition imposes increased requirements on pilots' situational awareness<sup>1,2</sup>, risk management<sup>3</sup>, and decision-making<sup>4,5</sup>. Flight missions frequently challenge pilots' cognitive talents and response capacities because of the interplay of technical faults, human errors, and complicated settings. Human factors have emerged as a primary contributor to aviation accidents<sup>6,7</sup>, underscoring the need for pilot selection, screening, and training in maintaining flight safety<sup>8</sup>.

Pilots, as a distinct professional category, experience a rigorous and controlled selection and training procedure. Pilot training is lengthy and costly and entails rigorous evaluations and possible disqualifications along the process, necessitating robust psychological, foundational, and behavioral competencies throughout the pilot's career<sup>9</sup>. Flight students must complete a series of intensive training courses to build operational skills and cognitive abilities necessary for managing various emergencies as the initial step toward becoming a professional pilot<sup>10</sup>. The psychomotor ability and learning adaptability of flight trainees are intricately connected to cerebral functioning systems<sup>11,12</sup>. Examining the mechanisms of brain functions associated with flight tasks executed by trainees is crucial for the safe operation of aircraft, as it offers objective physiological metrics for assessing and

<sup>1</sup>Institute of Flight Technology, Civil Aviation Flight University of China, Guanghan 618307, China. ✉email: yandongfeng@cafuc.edu.cn

evaluating flight trainees, thereby enhancing the selection and training system for pilots and addressing the new mandates from the Civil Aviation Administration regarding pilot training reform<sup>9</sup>.

Resting-state functional magnetic resonance imaging (resting-state fMRI) offers insight into the brain's intrinsic network connection characteristics. The human brain constitutes a vast interconnected network<sup>13</sup> with three principal neurocognitive networks: default mode network (DMN), central executive network (CEN), and salience network (SN)<sup>14–16</sup>. The interconnections among the DMN, CEN, and SN are essential for higher-order cognition and goal-directed behavior, including perceptual decision-making, emotional regulation, and attention allocation. The DMN exhibits heightened activity during rest and is comparatively diminished during cognitive tasks or external stimuli<sup>16,17</sup>, and it is engaged in self-centered, internally focused cognitive processes<sup>18</sup>. The primary regions encompass the medial prefrontal cortex, the posterior cingulate cortex, the precuneus, and the bilateral parietal cortex<sup>19</sup>. Previous research has demonstrated enhanced functional connections in the DMN of pilots<sup>20</sup>. The CEN's core regions include the bilateral dorsolateral prefrontal cortex and posterior parietal cortex<sup>21</sup>, exhibiting increased activity during activities related to attention management and decision-making<sup>22–24</sup>. The SN, involved in processing external stimuli and internal emotional fluctuations, assists the brain in identifying and filtering significant information<sup>16,25</sup>, with critical nodes in the dorsal anterior cingulate cortex and bilateral insula cortex<sup>21,26</sup>.

Efficient coordination between the DMN and the CEN enables individuals to equilibrate task performance and resting states<sup>27</sup>. Simultaneously, the SN is integral to the dynamic interactions between the DMN and CEN<sup>26,28</sup>. These three networks are essential components of the brain's triple-network model, which is crucial in diseases such as schizophrenia<sup>29,30</sup>, depression<sup>31,32</sup>, and autism spectrum disorder<sup>33,34</sup>. Examining the functional connectivity between these networks establishes a basis for comprehending brain mechanisms. Furthermore, emerging studies suggest that functional connectivity displays time-varying characteristics<sup>35,36</sup>, thereby highlighting dynamic functional network connectivity (dFNC). The dFNC methodology accounts for variations in functional connectivity at more granular time scales, yielding a more precise representation of the functional coordination among distinct brain regions<sup>37,38</sup>. The dFNC method facilitates accurate monitoring of alterations in functional connectivity among the triple networks.

Previous studies utilizing resting-state fMRI have shown that pilots' brain functional structures change after long-term flight training compared to individuals in other professions. Xu et al.<sup>39</sup> found that signals at low frequencies of pilots exhibited significant differences in the left cuneiform lobe and right cerebellum, with enhanced spontaneous activities in regions associated with visual processing and body balance. Radstake et al.<sup>40</sup> compared the brain functional connectivity data of pilots and non-pilots, discovering alterations in pilots' vestibular, motor, and multisensory processing regions. Jiang et al.<sup>41</sup> reported that effective connectivity between the right supramarginal gyrus and the right lingual gyrus was lower in pilots, indicating more excellent emotional stability in pilots under stimulation. Additionally, Chen et al.<sup>42</sup> reported elevated functional links among the triple networks in pilots, alongside reduced connection within CEN. In summary, current research has predominantly concentrated on senior pilots, thereby imposing constraints on sample selection. Moreover, while certain studies have employed the dFNC method to examine functional and structural brain differences between pilots and healthy controls, they have failed to correlate temporal metrics with behavioral test data. This constrains the capacity to investigate the precise relationships between pilots' memory, decision-making, and visual processing and their neural activity.

In contrast to general college students, flight trainees engage in consistent theoretical education and participate in diverse practical flight training programs, including flight simulators and aircraft training, to acquire their pilot license. Consequently, this research selected flight trainees and general college students enrolled during the same period and without any flight experience, as participants. Employing the dFNC analysis method, the research investigated the time-varying functional connection characteristics within triple neural networks (DMN, CEN, SN) during the resting state in both groups. Furthermore, the study integrated behavioural test data with temporal metrics to conduct a more comprehensive examination of the cognitive and neural functional alterations in flight trainees.

## Materials and methods

### Participants

Participants were recruited from the Civil Aviation Flight University of China, adhering to the following inclusion criteria: (1) male; (2) aged 21 to 25 years; (3) right-handed; (4) no metal implants in the body; (5) at the point of the experiment in decent physical health; (6) holding a bachelor's degree in engineering; (7) no history of mental illness; (8) no drug or alcohol dependence; (9) no history of traumatic brain injury, cerebrovascular disease, or chronic pain; and (10) voluntarily participated and signed the informed consent before involvement.

All participants underwent behavioral assessments, including the Berg Card Sorting Test (BCST) and the Change Detection Test, prior to MRI data collection. Following screening, data from 76 participants were incorporated into the study, comprising 39 flight trainees and 37 general college students who served as the control group. All flight trainees had fulfilled a minimum of 235 hours of flight training mandated by their flight academy and had acquired private and commercial pilot licenses issued by the Civil Aviation Administration of China, thereby qualifying them to operate small aircraft autonomously. This study adhered to the principles of the Declaration of Helsinki. It was approved by the Ethics and Human Protection Committee of the MRI Research Center at the University of Electronic Science and Technology of China, approval number 1420200408-07.

### Data acquisition

Magnetic resonance imaging (MRI) data collection was conducted at the Magnetic Resonance Imaging Center of the University of Electronic Science and Technology of China, using a GE Discovery MR750 3.0T

MRI scanner equipped with an 8-channel phased array head coil. T1 images were acquired utilizing a three-dimensional spoiled gradient echo sequence with the following parameters: repetition time (TR)=5.952 ms; echo time (TE)=1.964 ms; flip angle=9°; scan matrix=256×256; field of view (FOV)=256 mm × 256 mm; slice thickness=1.0 mm, and a total of 154 slices. Functional MRI (fMRI) data were acquired using a standard gradient echo pulse sequence with the following parameters: TR=2000 ms; TE=30 ms; flip angle=90°; scan matrix=64×64; FOV=240 mm × 240 mm; slice thickness=4.0 mm (with a 0.4 mm gap); a total of 35 slices; a scan duration of 510 s; and a total of 255 frames collected. Before the scan, participants were directed to eliminate all metallic items and don noise-cancelling earplugs. Participants were advised to maintain their eyes closed, remain awake, and refrain from contemplating particular tasks during the scan. Foam pads were positioned on either side of the participants' heads to restrict head movement.

### Data processing

Figure 1 illustrates that the data processing procedure comprised the following steps:

**Data Preprocessing:** Resting-state fMRI data were preprocessed using the RESTplus software (<http://restfmri.net>) within the Matlab 2022b platform. The preprocessing procedures were listed below: (1) removal of the initial five time points to reduce the influence of the magnetic field; (2) slice-timing correction; (3) head motion correction, with exclusion of any sample exhibiting head translation > 2 mm or rotation > 2°; (4) spatial normalization, where each individual's fMRI images were first registered to their corresponding sMRI images, followed by nonlinear registration to the Montreal Neurological Institute (MNI) space; (5) smoothing using a Gaussian kernel with a full width at half-maximum (FWHM) of 6 mm.

**Independent Component Analysis (ICA).** Group ICA was performed by GIFT software (<http://icatb.sourceforge.net/>)<sup>43</sup>. First, the number of independent components (ICs) was determined using the minimum description length (MDL) criteria<sup>44</sup>. Next, principal component analysis (PCA) was applied, followed by IC estimation using the Infomax algorithm. The procedure was executed 100 times in ICASSO (<http://research.ics.tkk.fi/ica/icasso/>), and 30 ICs were decomposed. Finally, the spatial distribution and time course of each IC were reconstructed with a back-reconstruction algorithm, and the group-independent spatial maps were scaled to Z-scores<sup>45</sup>.

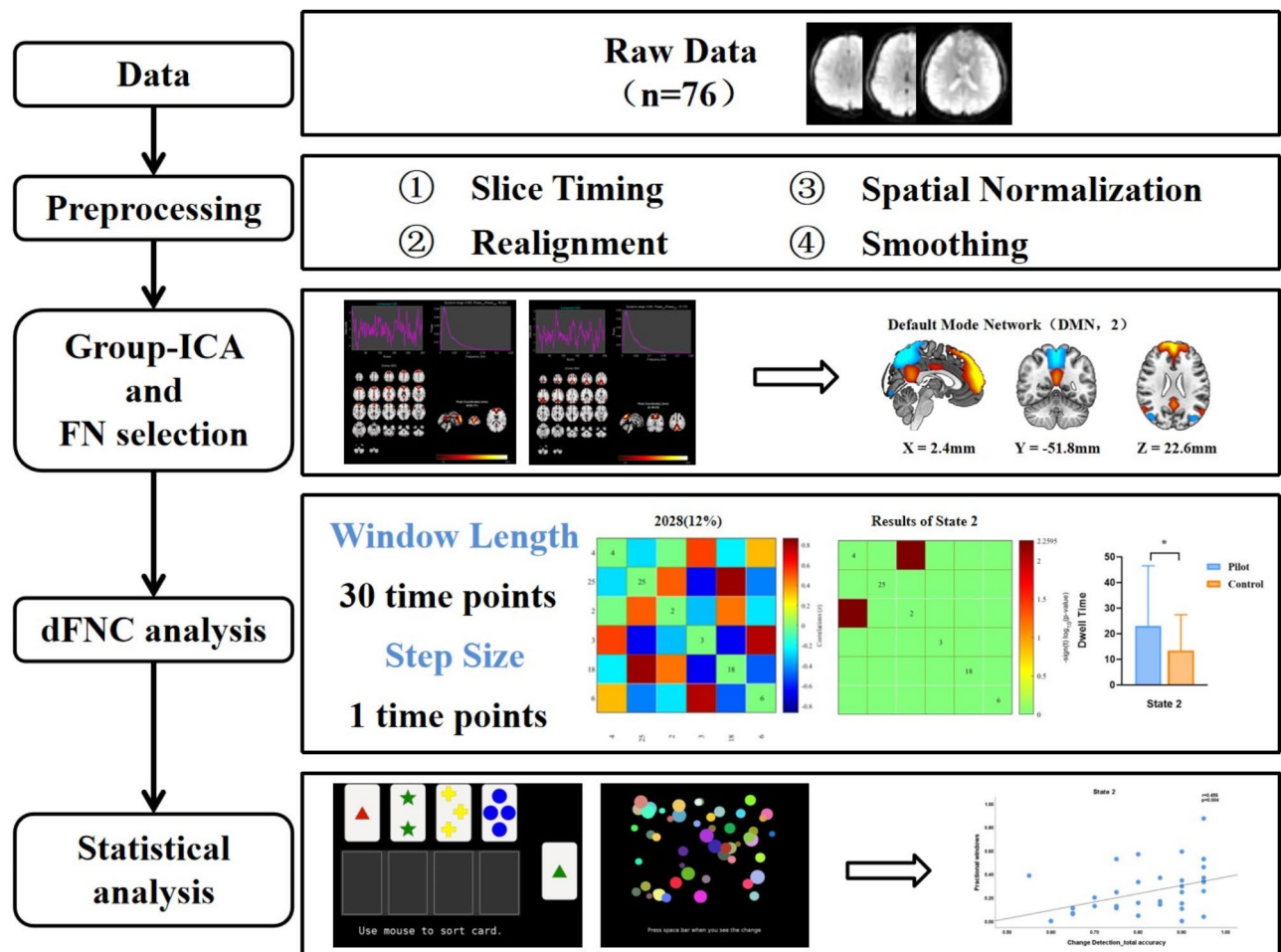


**Fig. 1.** Data processing workflow. Independent component analysis, sliding window, and K-means clustering techniques were employed to compute dFNC.

Selection of network components. The selection criteria for ICs were as follows: (1) high spatial similarity to the Stanford functional Regions of Interest (ROI) template; (2) peak activations primarily located in gray matter, with low spatial overlap with known artifacts such as blood vessels, ventricles, or susceptibility artifacts<sup>46,47</sup>; (3) power spectra dominated by low-frequency fluctuations. The chosen triple network components were then denoised through post-processing steps<sup>46,48–50</sup>, including regressing out six head motion parameters, removing trends (linear, quadratic, cubic), and applying a high-frequency cutoff of 0.15 Hz.

dFNC Analysis. The construction of dFNC applied a sliding time-window methodology. The steps were as follows: (1) the window size was set to 30 TRs (60s), with a step size of 1 TR (2s)<sup>51</sup>. Based on the least absolute shrinkage and selection operator (LASSO) framework, the regularized precision matrix was computed. An additional L1 norm constraint was applied to encourage sparsity. Each subject ultimately obtained 220 dFNC matrices, which were subsequently normalised employing Fisher's Z transformation; (2) clustering was performed utilizing the K-means algorithm and the Manhattan distance (with 1000 iterations and 150 repetitions). The optimal number of clusters,  $k=6$ , was determined using the elbow criterion<sup>52,53</sup>, representing six distinct functional connectivity states; (3) intergroup differences in dFNC strength between different states were compared with the false discovery rate (FDR) correction applied. Differences with a threshold of  $P<0.05$  were considered statistically significant<sup>54</sup>; (4) temporal properties were calculated, including fractional windows (percentage of each state among six states), mean dwell time (average time spent within a given state), and transition number (frequency of transitions between states throughout the entire time series).

Statistical analysis

Statistical analysis was performed using SPSS 26.0 software (<https://www.ibm.com/support/pages/download-ibm-spss-statistics-26-end-support-30-sep-2025>). The depiction of continuous data differed according to distribution. For regularly distributed data, descriptive statistics are represented as mean  $\pm$  standard deviation (SD), and an independent sample t-test was utilized. Data not distributed normally was displayed as the median (quartile) and evaluated via the Mann-Whitney U test. Categorical variables were presented as counts, and differences were considered statistically significant at  $P<0.05$ .

The Stats module of the GIFT software (<http://icatb.sourceforge.net/>) was used to analyze group differences in FNC matrices between flight trainees and controls in different states via two-sample t-tests. Differences were considered statistically significant at  $P<0.05$  (with FDR correction). The temporal properties were assessed by calculating fractional windows, mean dwell time, and transition numbers.

Spearman correlation analysis was employed to examine the relationship between notable temporal properties and behavioral test outcomes (BCST and Change Detection Test), with a threshold set at  $P<0.05$ . The BCST tasked participants with sorting cards based on shifting rules (e.g., color, shape, number). Measures including overall accuracy, perseverative responses (PR), perseverative errors (PE), and mean reaction time were collected to assess cognitive adaptability in response to environmental demands<sup>54</sup>. PR refers to cases in which participants continue using a rule despite knowing it is incorrect; PE refers to the inability of subjects to abandon the original classification principle after a change in categorization criteria, continuing to classify based on the previous principle<sup>10</sup>. The Change Detection Test presented a series of visual stimuli, and participants were required to judge whether any changes occurred between presentations<sup>55</sup>. The accuracy and mean reaction time were collected to evaluate visual memory retention and attentional allocation performance.

Results

Participants

The differences in age, gender, years of education, right-handedness, and flight hours between two groups were not statistically significant ( $P\geq0.05$ ). Table 1 presents the demographic parameters for all subjects.

Networks of interests

Based on previous research and a template-matching approach, six independent components (ICs) were selected as intrinsic connectivity networks. These six ICs were categorized into three distinct functional networks based on anatomical and other prior knowledge: the CEN, DMN, and SN. Figure 2 illustrates the spatial distribution of the six ICs within the CEN, DMN, and SN functional networks.

Using the MRICRON medical imaging analysis software (<http://www.nitrc.org/projects/mricron>) and prior knowledge from relevant fields, the brain regions corresponding to these six ICs, which are classified into the CEN, DMN, and SN functional domains, were surveyed. Functional network regions were assigned according to the MNI coordinate system (x, y, z). Detailed information on the functional networks, brain region names, IC numbers, and MNI peak coordinates for the six ICs is provided in Table 2.

Condition	Flying trainees( $n=39$ )	Controls( $n=37$ )	P value
Age(years)	22.85 $\pm$ 0.96	22.38 $\pm$ 0.92	0.49
Gender(male/female)	39/0	37/0	-
Education(years)	16	16	-
Handedness(% right)	100	100	-
Total flight hours(hours)	240.56 $\pm$ 8.74	-	-

Table 1. Demographic information was compared between the two groups.

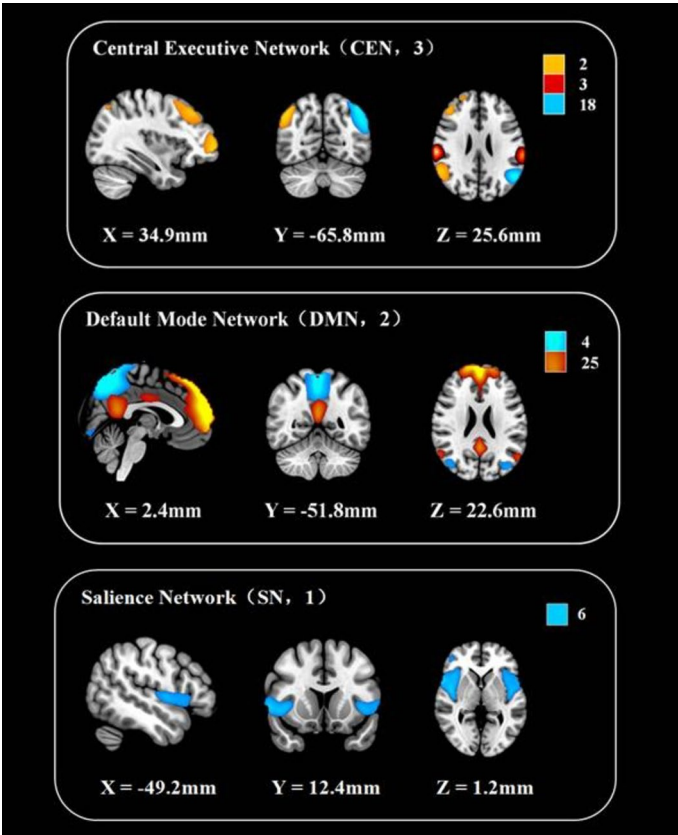


Fig. 2. Spatial maps of the selected six ICs.

Network	Brain regions (AAL)	IC number	Center(MNI)		
			x	y	z
Central Executive Network(CEN)	Right Supramarginal gyrus	2	54	-51	36
	Left Inferior Parietal Lobe	3	-63	-30	27
	Left Supramarginal gyrus	18	-51	-60	30
Default Mode Network(DMN)	Left Precuneus	4	-3	-63	57
	Left Superior Frontal Gyrus	25	-3	54	33
	Right Superior Frontal Gyrus	25	3	57	30
Salience Network(SN)	Left Insula	6	-45	-9	3
	Right Insula	6	45	-6	3

Table 2. Detailed information of the six components.

Differences between groups in the dFNC

During the acquisition of resting-state fMRI signals, six states were identified, each reflecting a distinct pattern of functional connectivity among diverse networks. The six functional connectivity matrices illustrated the fraction of each centroid and the intensity of functional connection during signal capture (as depicted in Fig. 3). Significant group differences were observed only in State 2 (Fig. 4). The flight trainees exhibited markedly improved functional connectivity linking the CEN and the DMN networks (IC2 and IC4,  $P<0.05$ , FDR corrected). Significant variations in brain regions were detected, as illustrated in Fig. 5.

The temporal metrics for six states were assessed by the Mann-Whitney U test. In State 2, flight trainees exhibited an increase in fractional windows ( $P=0.009$ ) and mean dwell time ( $P=0.029$ ), while in State 5 they showed a decrease in fractional windows ( $P=0.008$ ). However, no significant group differences were found in the transition number. Figure 4 presents the differences in dFNC metrics between groups, where \* indicates  $P<0.05$  after FDR correction.

Correlation analysis results

An analysis of the BCST revealed that the flight trainee group exhibited a significantly higher accuracy rate ( $P<0.05$ ), while reaction time, PR, and PE did not exhibit any substantial differences between groups.



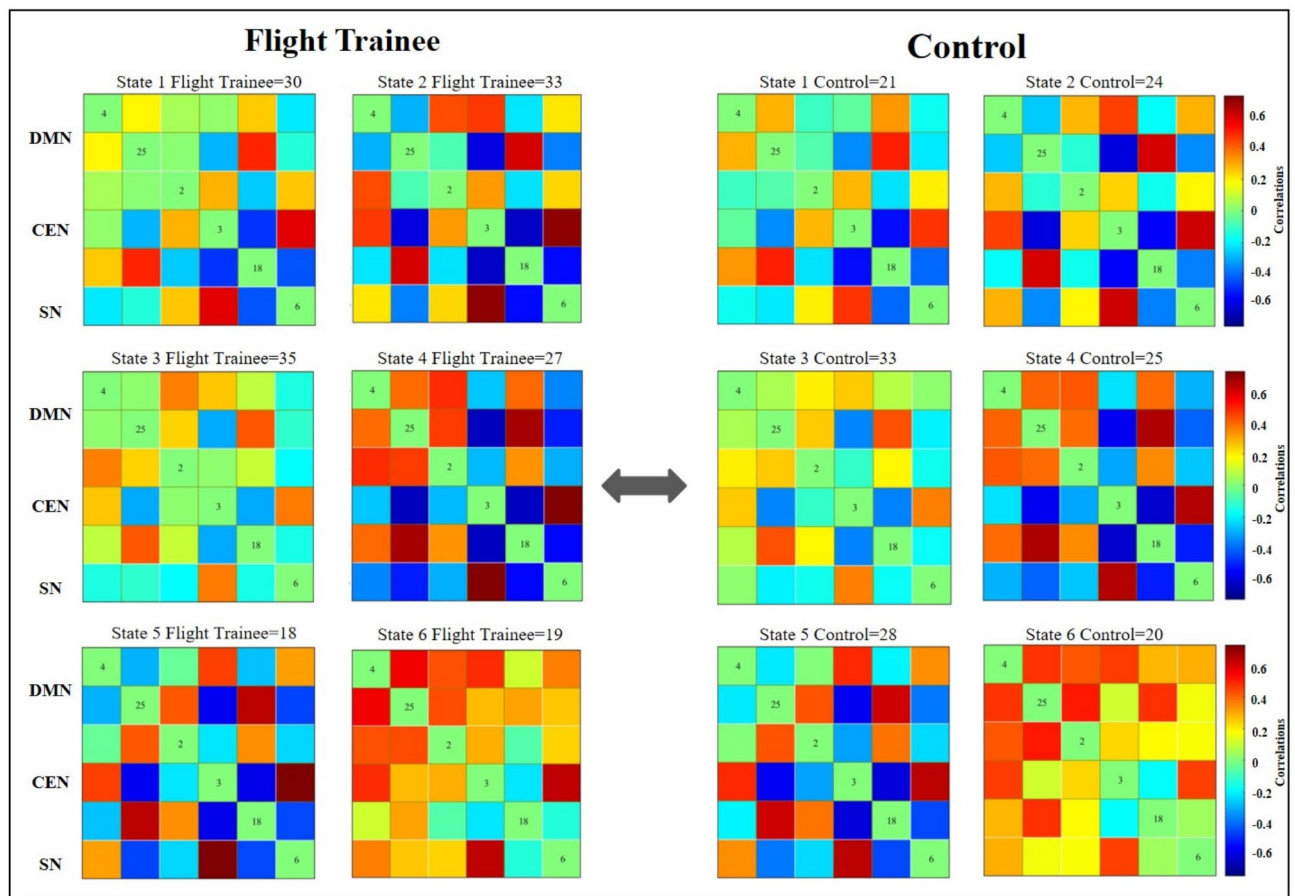


**Fig. 3.** The median connectivity matrices (centroid) of six states. The differences in the dynamic functional connectivity strength were depicted.

Furthermore, no substantial disparities were identified in the Change Detection Test with respect to reaction time or accuracy, as detailed in Table 3.

The correlation results demonstrated that, in State 2, the fractional windows in the flight trainee group were substantially positively correlated with BCST accuracy ( $r = 0.438$ ,  $P = 0.005$ ) and Change Detection Test accuracy ( $r = 0.456$ ,  $P = 0.004$ ). Similarly, the mean dwell time in State 2 was significantly positively correlated with BCST accuracy ( $r = 0.354$ ,  $P = 0.027$ ) and Change Detection Test accuracy ( $r = 0.348$ ,  $P = 0.032$ ). Nevertheless, no correlations were identified regarding the fractional windows in State 5 and the behavioral test data. The correlations between temporal metrics in State 2 and the behavioral test data for the flight trainee group are shown in Fig. 6.

## Discussion

This study identified six components and three resting-state networks through ICA, then estimated six states utilizing a sliding time-window approach and K-means clustering. The fractional windows and mean dwell time in State 2 were considerably distinct between the flight trainee and control groups. Additionally, the accuracies in the Berg Card Test and the Change Detection Test were highly correlated with both indicators in State 2 of the flight trainee group. Furthermore, significant differences in fractional windows were observed in State 5.

In State 2, enhanced functional connectivity between the CEN and DMN was observed within flight trainees, aligning with the findings of Chen et al.<sup>42</sup>. The CEN plays a crucial role in numerous intricate cognitive activities, such as attention allocation, visual processing, and emotional regulation<sup>56</sup>. Simultaneously, the DMN consolidates information from multiple regions<sup>57,58</sup>. Previous studies have demonstrated the cooperative involvement of these two networks during semantic processing tasks<sup>56,59</sup>, enabling efficient information processing and cognitive control. Additionally, long-term cognitive training may facilitate interaction between the DMN and CEN<sup>60</sup>. The enhanced functional connectivity linking the CEN and DMN in flight trainees may indicate that their brains have developed greater flexibility in allocating cognitive resources when handling complex tasks due to flight training. Flight tasks often require rapid switching between multiple tasks, with a high level of focus and vigilance. For instance, when navigation or instrument monitoring is needed, the CEN is likely dominant, whereas, during lower-demand tasks, the DMN might briefly take over for memory retrieval or decision-making. This flexible network switching allows pilots to optimize cognitive control, reduce unnecessary cognitive load, and improve the accuracy and efficiency of task execution.

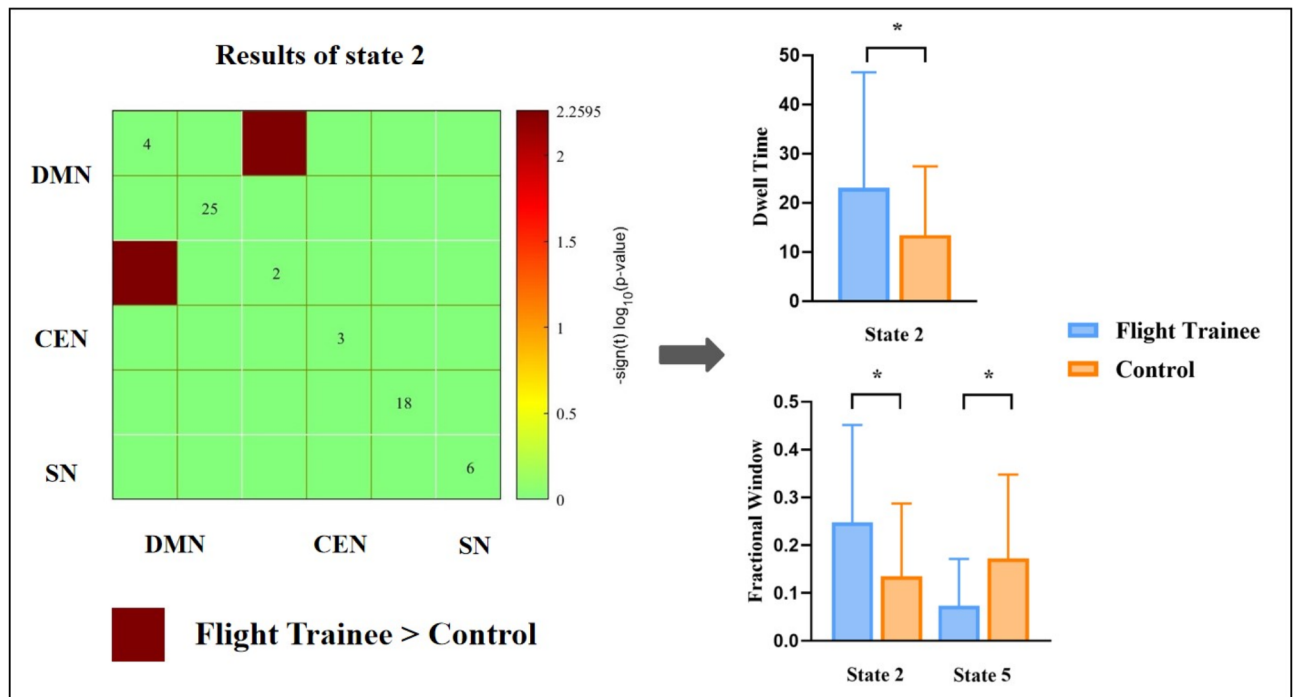


**Fig. 4.** dFNC and temporal metrics were found to differ between groups. Significant between-group comparisons for dFNC were reported only in State 2 ( $P < 0.05$ , FDR correction). Bar graphs illustrate the temporal metrics with substantial variations ( $P < 0.05$ ).

The temporal properties are intricately linked to multiple cognitive domains, including visuospatial ability, information transmission efficiency, and memory function<sup>49</sup>. An extended mean dwell time generally indicates enhanced stability of brain functional connectivity states. Research has shown that, after long-term training, taxi drivers exhibit a notable enhancement in mean dwell time within highly interconnected states associated with vigilance<sup>61</sup>. Conversely, cognitive impairments are frequently linked to prolonged mean dwell time in poorly interconnected states, as observed in individuals with Alzheimer's disease<sup>62</sup>, diabetes<sup>63</sup>, and depression<sup>64</sup>, who tend to spend more time in weakly connected states, manifesting symptoms such as inattention and reduced cognitive processing efficiency. The fractional windows reflect the extent to which individuals prefer to remain in a specific state. In closely connected states associated with efficient information processing and cognitive regulation, a higher fractional window generally signifies superior cognitive performance in complicated tasks. In this study, the flight trainees exhibited significantly increased fractional windows and mean dwell time in State 2 (characterized by enhanced functional connectivity between the CEN and DMN). In contrast, fractional windows in State 5 decreased. State 5 is characterized by "sparse connectivity"<sup>65</sup>, where most within- and between-network connections weaken, reducing information transmission efficiency to conserve energy<sup>66</sup>. Flight training is a multifaceted and evolving process necessitating flight trainees to consistently adjust to novel flight situations and task requirements. This adaptability may be shown in alterations in dynamic functional connectivity (dFC). After long-term flight training, the brain of the flight trainee group has adapted to the demands of intricate tasks, as evidenced by the increased fractional windows and mean dwell time in highly efficient functional connectivity states, such as State 2. The alterations in brain networks may indicate the flight trainees' enhanced capacity for stable and efficient information processing, as well as improved cognitive control when confronted with intricate tasks.

Additionally, this study utilized the BCST to assess three core cognitive components: cognitive flexibility, reasoning ability, and executive function. First, individuals are required to switch quickly between different rules; second, they are tested on their ability to identify relationships between cards through observation, comparison, and reasoning; and finally, they must maintain the current task goal while responding to changing rules, reflecting their executive function<sup>67</sup>. The overall accuracy of the test reflects an individual's executive ability level, with a higher precision indicating a more muscular executive function. The Change Detection Test, on the other hand, was used to explore visual working memory and attention resource allocation mechanisms. Higher overall accuracy in this test indicates greater ability to process visual information quickly. The results indicated that the increase in fractional windows and mean dwell time in State 2 was positively correlated with BCST and Change Detection Test accuracy in the flight trainee group. Additionally, the flight trainees performed better in executive function and visual working memory. State 2 is characterized by enhanced functional connectivity between the CEN and DMN, alongside elevated fractional windows and mean dwell time. This suggests that State 2 is a crucial state for capturing the effects of training, with brain functional connectivity in this state closely related to cognitive performance in flight trainees. In this state, flight trainees exhibited greater cognitive

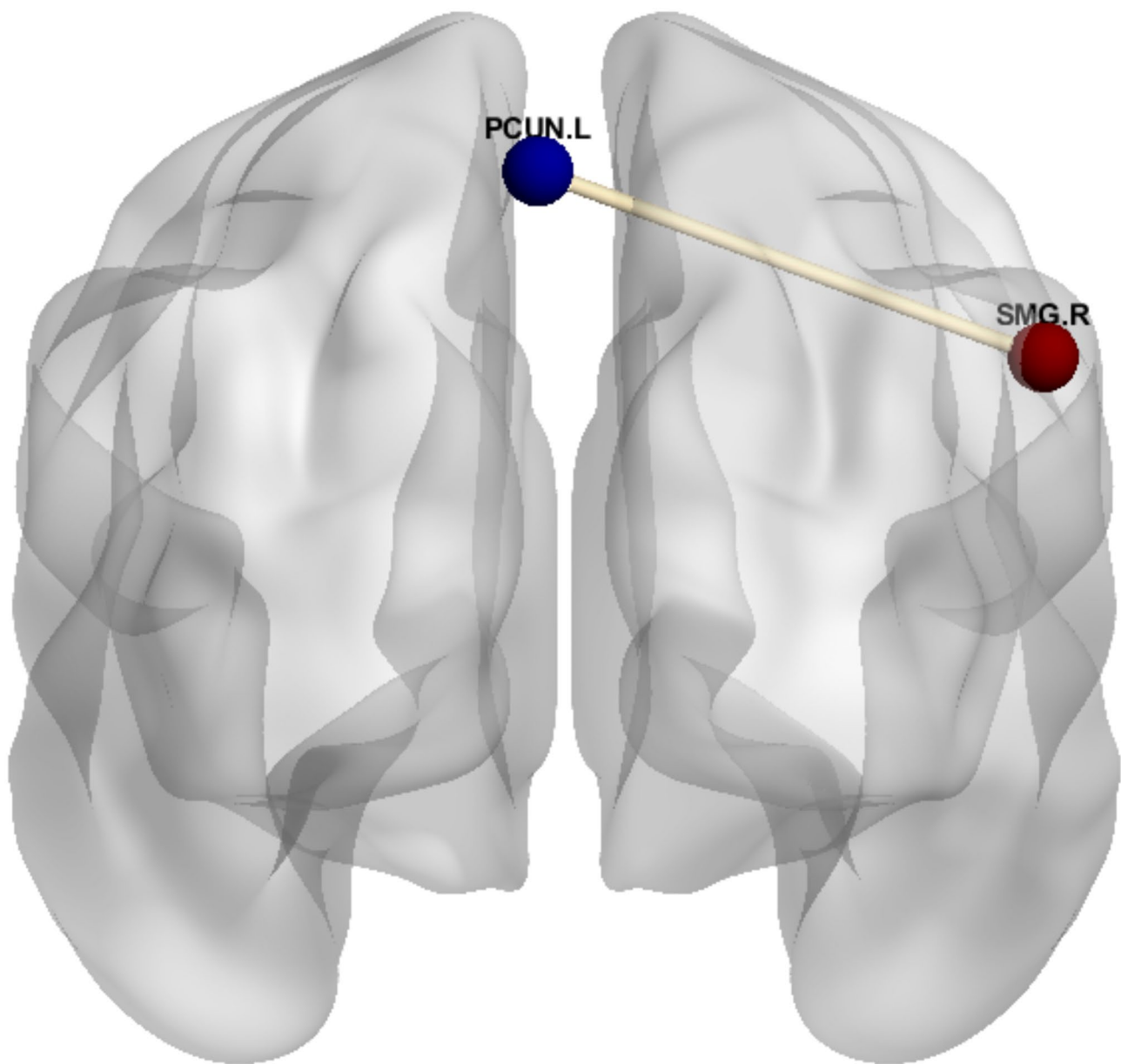


**Fig. 5.** Visualization of regions with significant differences. Red spheres indicate the right supramarginal gyrus, and blue spheres indicate the left precuneus. Yellow lines indicate enhanced functional connectivity in the flight trainee group. Each state required at least 10 windows per participant to be included in the analysis.

	Flight Trainees( <i>n</i> = 39)	Controls( <i>n</i> = 37)	T value	P value
BCST_total accuracy(%)	78.97 ± 7.32	71.79 ± 13.47	2.86	0.01
BCST_perseverative response	18.08 ± 4.86	16.70 ± 5.58	1.15	0.26
BCST_perseverative error	7.03 ± 3.18	6.86 ± 3.08	0.22	0.82
BCST_reaction time(s)	1.90 ± 0.60	1.99 ± 1.46	-0.36	0.72
Change Detection Test _ total accuracy(%)	82.05 ± 12.34	78.92 ± 13.34	1.06	0.29
Change Detection Test _ reaction time(s)	20.70 ± 6.48	18.51 ± 6.07	1.52	0.13

**Table 3.** Characteristics of the flight trainee and control groups.



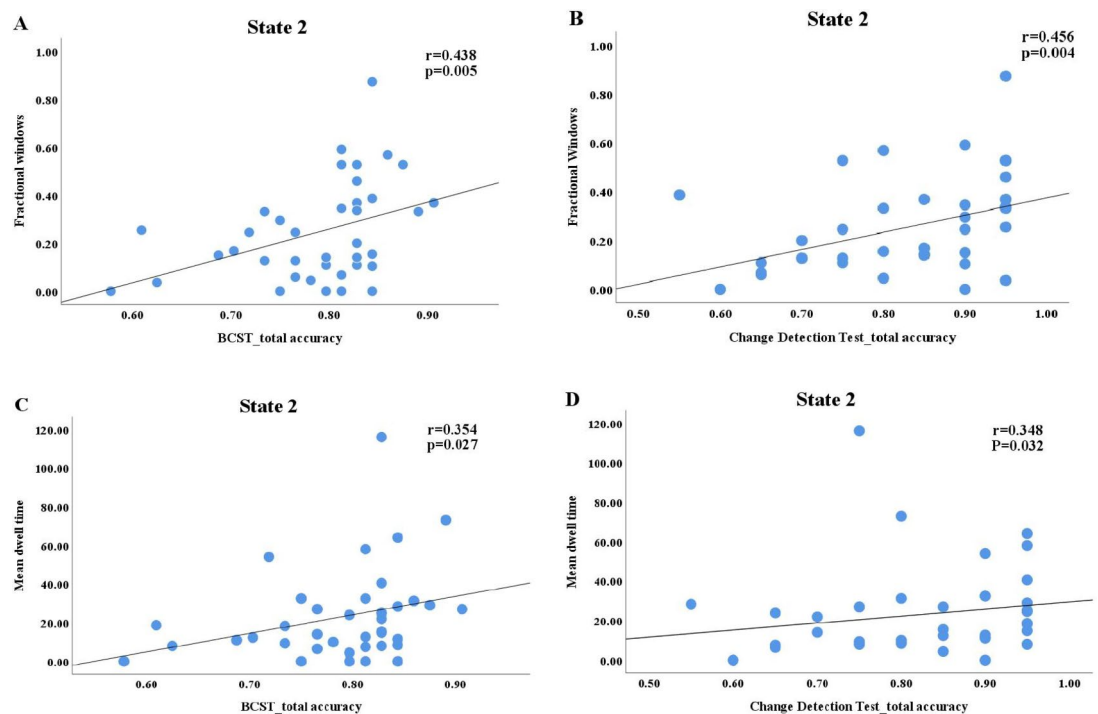


**Fig. 6.** Correlation analysis results. (A-B) Correlation between fractional windows in State 2 and BCST, Change Detection Test accuracy. (C-D) Correlation between mean dwell time in State 2 and BCST, Change Detection Test accuracy.

flexibility, information integration ability, and visual processing capability, which may be associated with flight training. Through intensive simulator training and real flight missions, flight training enhances the ability to monitor instrument information, continuously strengthening various cognitive functions such as information perception and integration, attention, and decision-making in flight trainees. Particularly during takeoff and landing phases, the improved ability to track moving objects and perceive acceleration sharpens flight trainees' brain function and visual processing capabilities. After long-term training, flight trainees may develop stronger functional connectivity in specific states, along with higher fractional windows and mean dwell time, leading to improved visual processing and cognitive control abilities. This also reflects the brain's enhanced adaptability following training.

However, this study has several limitations, including the relatively small sample size. Future research could overcome these limitations by increasing the sample size, employing different window sizes, and conducting graph theory analyses better to observe changes in brain functional connectivity among flight trainees. This could help explore quantifiable physiological indicators for evaluating and assessing pilots in this unique profession.

## Conclusion

This study utilized dFNC analysis to reveal the dynamic functional connectivity pattern changes among flight trainees, primarily manifested as increased functional connectivity between the DMN and CEN in flight trainees. Flight trainees exhibited significantly increased fractional windows and mean dwell time in State 2, along with a reduction in fractional windows in State 5. Additionally, in State 2, both differential temporal metrics of flight trainees exhibited a positive correlation with BCST and Change Detection Test performance. These differences may indicate that, following flight training, the flight trainees exhibited enhanced coordination between the DMN and CEN regions, which are associated with cognitive performance, along with more stable functional connectivity states, greater cognitive flexibility, improved information integration, and enhanced visual processing capabilities. The findings suggest that dFNC analysis can capture more subtle changes in brain network connectivity in flight trainees, providing valuable insight into brain functional changes following flight training. Moreover, dFNC may serve as a useful physiological indicator for monitoring brain function.

## Data availability

The data from this study are available upon request due to legal restrictions. The sharing of physiological data from pilots is prohibited by the Civil Aviation Administration of China. Researchers interested in accessing the data may contact: yandongfeng@cafuc.edu.cn.

Received: 4 November 2024; Accepted: 3 February 2025

Published online: 06 March 2025

## References

- Gao, L., Wang, C. & Wu, G. Hidden Semi-markov models-based visual Perceptual State Recognition for pilots. *Sensors* **23**, 6418. <https://doi.org/10.3390/s23146418> (2023).
- Yiu, C. Y. et al. Towards safe and collaborative aerodrome operations: assessing shared situational awareness for adverse weather detection with EEG-enabled bayesian neural networks. *Adv. Eng. Inform.* **53**, 101698. <https://doi.org/10.1016/j.aei.2022.101698> (2022).
- Sun, J. Y. & Sun, R. S. Pilot fatigue survey: a study of the mutual influence among fatigue factors in the work dimension. *Front. Public Health*. **11** <https://doi.org/10.3389/fpubh.2023.1014503> (2023).
- Martins, A., Köbrich, M., Carstengerdes, N. & Biella, M. All's well that ends well? Outcome Bias in Pilots during Instrument Flight rules. *Appl. Cogn. Psychol.* **37**, 433–442. <https://doi.org/10.1002/acp.4046> (2023).
- Beling, C. & Wild, G. The association between emotional intelligence and decision making for pilots. *J. Air Transp. Manage.* **114** <https://doi.org/10.1016/j.jairtraman.2023.102506> (2024).
- Oraith, H., Blanco-Davis, E., Yang, Z. & Matellini, B. An evaluation of the effects of Human factors on Pilotage Operations Safety. *J. Mar. Sci. Appl.* **20**, 393–409 (2021).
- Masi, G., Amprimo, G., Ferraris, C. & Priano, L. Stress and workload Assessment in Aviation—A narrative review. *Sensors* **23**, 3556 (2023).
- Kelly, D. & Efthymiou, M. An analysis of human factors in fifty controlled flight into terrain aviation accidents from 2007 to 2017. *J. Saf. Res.* **69**, 155–165. <https://doi.org/10.1016/j.jsr.2019.03.009> (2019).
- Implementation Roadmap for the Construction of the Professionalism Lifecycle Management System for Civil Aviation Transport Pilots in China, (2020). [https://www.caac.gov.cn/XXGK/XXGK/ZCFB/202012/t20201225\\_205785.html](https://www.caac.gov.cn/XXGK/XXGK/ZCFB/202012/t20201225_205785.html) (In Chinese).
- Chen, X. et al. Flight training changes the brain functional pattern in cadets. *Front. NeuroSci.* **17** <https://doi.org/10.3389/fnins.2023.1120628> (2023).
- Mark, J. A., Ayaz, H. & Callan, D. E. Simultaneous fMRI and tDCS for enhancing training of Flight tasks. *Brain Sci.* **13** <https://doi.org/10.3390/brainsci13071024> (2023).
- Chen, X., Chu, Q., Meng, Q. B., Xu, P. R. & Zhang, S. C. Alterations in white matter fiber tracts and their correlation with flying cadet behavior. *Cereb. Cortex*. **34** <https://doi.org/10.1093/cercor/bhad548> (2024).
- Bressler, S. L. & Menon, V. Large-scale brain networks in cognition: emerging methods and principles. *Trends Cogn. Sci.* **14**, 277–290. <https://doi.org/10.1016/j.tics.2010.04.004> (2010).
- Jones, J. S., Monaghan, A., Leyland-Craggs, A., Astle, D. E. & Team, C. Testing the triple network model of psychopathology in a transdiagnostic neurodevelopmental cohort. *Neuroimage-Clinical* **40** <https://doi.org/10.1016/j.nicl.2023.103539> (2023).
- Corr, R. et al. Triple Network Functional Connectivity during Acute Stress in adolescents and the influence of polyvictimization. *Biol. Psychiatry-Cognitive Neurosci. Neuroimaging*. **7**, 867–875. <https://doi.org/10.1016/j.bpsc.2022.03.003> (2022).
- Menon, V. Large-scale brain networks and psychopathology: a unifying triple network model. *Trends Cogn. Sci.* **15**, 483–506. <https://doi.org/10.1016/j.tics.2011.08.003> (2011).
- Barch, D. M. Brain network interactions in health and disease. *Trends Cogn. Sci.* **17**, 603–605. <https://doi.org/10.1016/j.tics.2013.09.004> (2013).
- Rangel, A., Camerer, C. & Montague, P. R. A framework for studying the neurobiology of value-based decision making. *Nat. Rev. Neurosci.* **9**, 545–556. <https://doi.org/10.1038/nrn2357> (2008).
- Buckner, R. L., Andrews-Hanna, J. R. & Schacter, D. L. The brain's default network - anatomy, function, and relevance to disease. *Ann. N. Y. Acad. Sci.* **1124**, 1–38. <https://doi.org/10.1196/annals.1440.011> (2008).
- Chen, X. et al. Altered default Mode Network dynamics in Civil Aviation pilots. *Front. NeuroSci.* **13** <https://doi.org/10.3389/fnins.2019.01406> (2020).
- Seeley, W. W. et al. Dissociable intrinsic connectivity networks for salience processing and executive control. *J. Neurosci.* **27**, 2349–2356. <https://doi.org/10.1523/jneurosci.5587-06.2007> (2007).
- Müller, N. G. & Knight, R. T. The functional neuroanatomy of working memory:: contributions of human brain lesion studies. *Neuroscience* **139**, 51–58. <https://doi.org/10.1016/j.neuroscience.2005.09.018> (2006).
- Koechlin, E. & Summerfield, C. An information theoretical approach to prefrontal executive function. *Trends Cogn. Sci.* **11**, 229–235. <https://doi.org/10.1016/j.tics.2007.04.005> (2007).
- Menon, B. Towards a new model of understanding - the triple network, psychopathology and the structure of the mind. *Med. Hypotheses*. **133** <https://doi.org/10.1016/j.mehy.2019.109385> (2019).
- Uddin, L. Q. Salience processing and insular cortical function and dysfunction. *Nat. Rev. Neurosci.* **16**, 55–61. <https://doi.org/10.1038/nrn3857> (2015).
- Goulden, N. et al. The salience network is responsible for switching between the default mode network and the central executive network: replication from DCM. *NeuroImage* **99**, 180–190. <https://doi.org/10.1016/j.neuroimage.2014.05.052> (2014).
- Sridharan, D., Levitin, D. J. & Menon, V. A critical role for the right fronto-insular cortex in switching between central-executive and default-mode networks. *Proc. Natl. Acad. Sci. U.S.A.* **105**, 12569–12574. <https://doi.org/10.1073/pnas.080005105> (2008).
- Kim, A. et al. Triple-network dysconnectivity in patients with First-Episode Psychosis and individuals at clinical high risk for psychosis. *Br. Psychiatry Invest.* **19**, 1037–1045. <https://doi.org/10.30773/pi.2022.0091> (2022).
- Xi, Y. B. et al. Triple network hypothesis-related disrupted connections in schizophrenia: a spectral dynamic causal modeling analysis with functional magnetic resonance imaging. *Schizophr. Res.* **233**, 89–96. <https://doi.org/10.1016/j.schres.2021.06.024> (2021).
- Liang, S. G. et al. Aberrant triple-network connectivity patterns discriminate biotypes of first-episode medication-naïve schizophrenia in two large independent cohorts. *Neuropsychopharmacology: Official Publication Am. Coll. Neuropsychopharmacol.* **46**, 1502–1509. <https://doi.org/10.1038/s41386-020-00926-y> (2021).
- Li, Y. L., Dai, X., Wu, H. W. & Wang, L. J. Establishment of effective biomarkers for depression diagnosis with Fusion of multiple resting-state connectivity measures. *Front. NeuroSci.* **15** <https://doi.org/10.3389/fnins.2021.729958> (2021).
- Macêdo, M. A., Sato, J. R., Bressan, R. A. & Pan, P. M. Adolescent depression and resting-state fMRI brain networks: a scoping review of longitudinal studies. *Brazilian J. Psychiatry*. **44**, 420–433. <https://doi.org/10.47626/1516-4446-2021-2032> (2022).
- Guo, X. A. et al. Dysregulated dynamic time-varying triple-network segregation in children with autism spectrum disorder. *Cereb. Cortex*. **33**, 5717–5726. <https://doi.org/10.1093/cercor/bhac454> (2023).
- Wang, L. et al. Posterior default mode network is associated with the social performance in male children with autism spectrum disorder: a dynamic causal modeling analysis based on triple-network model. *Hum. Brain. Mapp.* **45** <https://doi.org/10.1002/hbm.26750> (2024).
- Tu, Y. H. et al. Abnormal thalamocortical network dynamics in migraine. *Neurology* **92**, 2706–2716. <https://doi.org/10.1212/wnl.000000000007607> (2019).
- Matsui, T. & Yamashita, K. Static and dynamic functional connectivity alterations in Alzheimer's Disease and Neuropsychiatric diseases. *Brain Connect.* **13**, 307–314. <https://doi.org/10.1089/brain.2022.0044> (2023).
- Yue, X. et al. Abnormal dynamic functional network connectivity in adults with Autism Spectrum Disorder. *Clin. Neuroradiol.* **32**, 1–10. <https://doi.org/10.1007/s00062-022-01173-y> (2022).
- Hu, Z. Y., Zhou, C. & He, L. C. Abnormal dynamic functional network connectivity in patients with early-onset bipolar disorder. *Front. Psychiatry*. **14** <https://doi.org/10.3389/fpsyt.2023.1169488> (2023).

39. Xu, K. et al. Research on brain functions related to visual information processing and body coordination function of pilots based on the low-frequency amplitude method. *Front. Hum. Neurosci.* **17** <https://doi.org/10.3389/fnhum.2023.796526> (2023).
40. Radstake, W. E. et al. Neuroplasticity in F16 fighter jet pilots. *Front. Physiol.* **14** <https://doi.org/10.3389/fphys.2023.1082166> (2023).
41. Jiang, H. et al. The neural underpinnings of emotional conflict control in pilots. *Aerosp. Med. Hum. Perform.* **91**, 798–805. <https://doi.org/10.3357/amhp.5618.2020> (2020).
42. Chen, X. et al. Increased functional dynamics in civil aviation pilots: evidence from a neuroimaging study. *PLoS One*. **15** <https://doi.org/10.1371/journal.pone.0234790> (2020).
43. Erhardt, E. B. et al. Comparison of multi-subject ICA methods for analysis of fMRI data. *Hum. Brain. Mapp.* **32**, 2075–2095. <https://doi.org/10.1002/hbm.21170> (2011).
44. Li, Y. O., Adali, T. & Calhoun, V. D. Estimating the number of independent components for functional magnetic resonance imaging data. *Hum. Brain. Mapp.* **28**, 1251–1266. <https://doi.org/10.1002/hbm.20359> (2007).
45. Wang, C. et al. Large-Scale Internetwork Functional Connectivity Mediates the Relationship between Serum Triglyceride and Working Memory in Young Adulthood. *Neural plasticity* 8894868 (2020).
46. Allen, E. A. et al. Tracking whole-brain connectivity dynamics in the resting state. *Cerebral cortex (New York, N.Y.: 24, 663–676, (1991).* <https://doi.org/10.1093/cercor/bhs352> (2014).
47. Shirer, W. R., Ryali, S., Rykhlevskaia, E., Menon, V. & Greicius, M. D. Decoding subject-driven Cognitive States with whole-brain connectivity patterns. *Cereb. Cortex.* **22**, 158–165. <https://doi.org/10.1093/cercor/bhr099> (2012).
48. Rashid, B., Damaraju, E., Pearson, G. D. & Calhoun, V. D. Dynamic connectivity states estimated from resting fMRI identify differences among Schizophrenia, bipolar disorder, and healthy control subjects. *Front. Hum. Neurosci.* **8** <https://doi.org/10.3389/fnhum.2014.00897> (2014).
49. Fiorenzato, E. et al. Dynamic functional connectivity changes associated with dementia in Parkinson's disease. *Brain* **142**, 2860–2872. <https://doi.org/10.1093/brain/awz192> (2019).
50. Yang, D. et al. Abnormal dynamic functional connectivity in young nondisabling intracerebral hemorrhage patients. *Ann. Clin. Transl. Neurol.* **11**, 1567–1578. <https://doi.org/10.1002/acn3.52074> (2024).
51. Wang, Y. et al. Altered static and dynamic functional network connectivity in primary angle-closure glaucoma patients. *Sci. Rep.* **14**, 11682. <https://doi.org/10.1038/s41598-024-62635-6> (2024).
52. Kim, J. et al. Abnormal intrinsic brain functional network dynamics in Parkinson's disease. *Brain* **140**, 2955–2967. <https://doi.org/10.1093/brain/awx233> (2017).
53. Yao, Z. J. et al. Altered dynamic functional connectivity in weakly-connected state in major depressive disorder. *Clin. Neurophysiol.* **130**, 2096–2104. <https://doi.org/10.1016/j.clinph.2019.08.009> (2019).
54. Fox, C. J., Mueller, S. T., Gray, H. M., Raber, J. & Piper, B. J. Evaluation of a short-form of the Berg Card sorting test. *PLoS One*. **8** <https://doi.org/10.1371/journal.pone.0063885> (2013).
55. Mueller, S. T. & Piper, B. J. The psychology experiment Building Language (PEBL) and PEBL test battery. *J. Neurosci. Methods.* **222**, 250–259. <https://doi.org/10.1016/j.jneumeth.2013.10.024> (2014).
56. Binder, J. R. & Desai, R. H. The neurobiology of semantic memory. *Trends Cogn. Sci.* **15**, 527–536. <https://doi.org/10.1016/j.tics.2011.10.001> (2011).
57. Cavanna, A. E. The precuneus and consciousness. *CNS Spectr.* **12**, 545–552. <https://doi.org/10.1017/s1092852900021295> (2007).
58. Zhang, S. & Li, C. S. R. Functional connectivity mapping of the human precuneus by resting state fMRI. *NeuroImage* **59**, 3548–3562. <https://doi.org/10.1016/j.neuroimage.2011.11.023> (2012).
59. Seghier, M. L. The angular Gyrus: multiple functions and multiple subdivisions. *Neuroscientist* **19**, 43–61. <https://doi.org/10.1177/1073858412440596> (2013).
60. Cao, W. F. et al. Effects of cognitive training on resting-state functional connectivity of default Mode, salience, and Central Executive Networks. *Front. Aging Neurosci.* **8** <https://doi.org/10.3389/fnagi.2016.00070> (2016).
61. Shen, H. et al. Changes in functional connectivity dynamics associated with vigilance network in taxi drivers. *NeuroImage* **124**, 367–378. <https://doi.org/10.1016/j.neuroimage.2015.09.010> (2016).
62. Schumacher, J. et al. Dynamic functional connectivity changes in dementia with Lewy bodies and Alzheimer's disease. *NeuroImage-Clinical* **22** <https://doi.org/10.1016/j.nicl.2019.101812> (2019).
63. Fu, L. Q. et al. Altered dynamics of Brain spontaneous activity and functional networks Associated with cognitive impairment in patients with type 2 diabetes. *J. Magn. Reson. Imaging.* **60**, 2547–2561. <https://doi.org/10.1002/jmri.29306> (2024).
64. Zheng, R. P. et al. Abnormal dynamic functional connectivity in first-episode, drug-naïve adolescents with major depressive disorder. *J. Neurosci. Res.* **100**, 1463–1475. <https://doi.org/10.1002/jnr.25047> (2022).
65. Wang, Y. Y. et al. An imbalance between functional segregation and integration in patients with pontine stroke: a dynamic functional network connectivity study. *NeuroImage-Clinical* **28** <https://doi.org/10.1016/j.nicl.2020.102507> (2020).
66. Gu, Y. et al. Abnormal dynamic functional connectivity in Alzheimer's disease. *CNS Neurosci. Ther.* **26**, 962–971. <https://doi.org/10.1111/cns.13387> (2020).
67. Dehaene, S. & Changeux, J. P. The Wisconsin Card sorting test: theoretical analysis and modeling in a neuronal network. *Cereb. Cortex.* **1**, 62–79. <https://doi.org/10.1093/cercor/1.1.62> (1991).

## Author contributions

L.Y. designed the experiments, wrote drafts of the paper, and approved the final draft; L.Y.B. collected and analyzed the data, authored drafts of the paper; D.F.Y. made contributions to the analysis and interpretation of the data. All authors contributed to and approved the final manuscript.

## Funding

This study was funded by the Fundamental Research Funds for the Central Universities (ZJ2023-013) and the Fundamental Research Funds for the Central Universities (J2023-004).

## Declarations

## Competing interests

The authors declare no competing interests.

## Ethics statement

The studies involving human participants were reviewed and approved by the Ethics Committee of the University of Electronic Science and Technology of China. The participants provided their written informed consent to take part in this study.

### Author contributions statement

L.Y. designed the experiments, wrote drafts of the paper, and approved the final draft; L.Y.B. collected and analyzed the data and authored drafts of the paper; D.F.Y. made contributions to the analysis and interpretation of the data. All authors contributed to and approved the final manuscript.

### Additional information

**Correspondence** and requests for materials should be addressed to D.Y.

**Reprints and permissions information** is available at [www.nature.com/reprints](http://www.nature.com/reprints).

**Publisher's note** Springer Nature remains neutral with regard to jurisdictional claims in published maps and institutional affiliations.

**Open Access** This article is licensed under a Creative Commons Attribution-NonCommercial-NoDerivatives 4.0 International License, which permits any non-commercial use, sharing, distribution and reproduction in any medium or format, as long as you give appropriate credit to the original author(s) and the source, provide a link to the Creative Commons licence, and indicate if you modified the licensed material. You do not have permission under this licence to share adapted material derived from this article or parts of it. The images or other third party material in this article are included in the article's Creative Commons licence, unless indicated otherwise in a credit line to the material. If material is not included in the article's Creative Commons licence and your intended use is not permitted by statutory regulation or exceeds the permitted use, you will need to obtain permission directly from the copyright holder. To view a copy of this licence, visit <http://creativecommons.org/licenses/by-nc-nd/4.0/>.

© The Author(s) 2025